Materials Transactions, Vol. 51, No. 6 (2010) pp. 1059 to 1063
©2010 The Japan Institute of Metals

Void Formation and Structure Change Induced by Heavy Ion Irradiation in GaSb and InSb

Noriko Nitta[1], Tokiya Hasegawa[1,*], Hidehiro Yasuda[1], Yoshihiko Hayashi[2], Toshimasa Yoshiie[2], Masafumi Taniwaki[3] and Hirotaro Mori[4]

[1]*Department of Mechanical Engineering, Kobe University, Kobe 657-8501, Japan*
[2]*Research Reactor Institute, Kyoto University, Sennan, Osaka 590-0494, Japan*
[3]*School of Environmental Science and Technology, Kochi University of Technology, Kami 782-8502, Japan*
[4]*Research Center for Ultra-High Voltage Electron Microscopy, Osaka University, Suita 565-0871, Japan*

Void formation and structure change by heavy ion irradiation were investigated in GaSb and InSb thin films. The voids were formed after irradiation in both materials. The average diameter of the voids was about 15 nm in GaSb and 20 nm in InSb irradiated with 60 keV Sn^+ ions to a fluence of 0.25×10^{18} ions/m^2 at room temperature. The void size in InSb is larger than that in GaSb. The large void size is quantitatively explained by the amount of induced vacancies obtained by the SRIM code simulation. The Debye-Scherrer rings were observed in the SAED patterns on both materials. The structure changes into a polycrystal by ion irradiation. Additionally, the 200 superlattice reflections in the [001] net pattern were almost absent, and the streak pattern along the $\langle 110 \rangle$ direction was observed in InSb. It is considered that the anti phase domains of different lengths are formed by ion irradiation. Ion irradiation transforms the structure of InSb from chemical ordering to chemical disordering via the formation of anti phase boundaries. [doi:10.2320/matertrans.M2010037]

(Received February 1, 2010; Accepted March 16, 2010; Published April 28, 2010)

Keywords: *gallium antimonide, indium antimonide, III-V compound semiconductor, thin foil irradiation, tin ion, void, point defects, vacancy, interstitial, transmission electron microscopy, anti phase boundary*

1. Introduction

Defect structure formation in III-V compound semiconductors induced by ion irradiation is classified into three categories. In the case of a typical defect structure, for example, GaAs[1–3] and InP,[4] a damaged layer corresponding to the projected ion range is formed on the surface by ion irradiation; further irradiation transforms the damaged layer into an amorphous structure. Si is an elemental semiconductor classified into this category. In the case of GaN,[5–8] nitrogen bubbles and gallium nanocrystals are formed in the amorphized layer by ion irradiation. In the case of GaSb[9–17] and InSb,[9,17,18] unusual behaviors, such as elevation, swelling, and the formation of holes, voids, nanofibers, and cellular structures with nano to submicron dimensions, are observed on irradiated surfaces. Similar phenomena occur in irradiated Ge surfaces (for example, see Refs. 19–27)). It is clarified that such anomalous phenomena occur as a result of the movement of point defects induced by ion irradiation, and these structures are generated after void formation. These phenomena have been reported in relation to bulk irradiation. Thin film irradiation will yield some useful knowledge on the movement of point defects utilizing surface sinks; however there are few studies on GaSb and InSb. In this study, void formation in the early stage of such structures and structure change by ion irradiation were investigated in GaSb and InSb thin films using transmission electron microscopy (TEM). In addition, structures formed in GaSb were compared with those formed in InSb in order to investigate the effect of the constituent elements.

*Graduate Student, Kobe University

2. Experimental Procedures

Single crystals of GaSb and InSb were supplied in the form of wafers 450 mm thick with the $\langle 001 \rangle$ normal. Discs of about 3 mm diameter were cut from the wafer, and a dimple was formed at the central portion of the discs. Then the disks were thinned by ion milling with argon for TEM observation. Sn^+ ion irradiation of 60 keV was performed for thin film using a heavy ion accelerator. The projected ion range was 25 nm in GaSb and 27 nm in InSb, obtained by the stopping and range of ions in matter (SRIM) code simulation.[28] The temperature of irradiation was 300 K. The ion fluence and flux were 0.25×10^{18}–2×10^{18} ions/m^2 and 3×10^{11} ions/m^{2}s, respectively. The observation was carried out with a transmission electron microscope (HITACHI H-7000 and HF-2000) operated at 125 kV and 200 kV.

3. Results and Discussion

Figure 1 shows TEM images (bright-field image) and their selected area electron diffraction (SAED) patterns of GaSb before and after irradiation. The direction of observation is [001]. The size of a SAED aperture is 1 μmϕ. Voids were formed in each sample after irradiation. The average diameter of the voids was about 14 nm in the sample irradiated to a fluence of 0.25×10^{18} ions/m^2 (Fig. 1(b)). The density of voids was 3×10^{15} voids/m^2. The swelling ratio of voids was 9% (a damage level of approximately 0.75 dpa). The diameter of voids grew to 23 nm in the sample irradiated to a fluence of 0.5×10^{18} ions/m^2 (Fig. 1(c)). The density of voids was 2×10^{15} voids/m^2. Despite the increasing ion fluence, the density decreased, which seems to be due to the coalescence of several voids. The swelling of voids increased up to 24% (a damage level of approx-

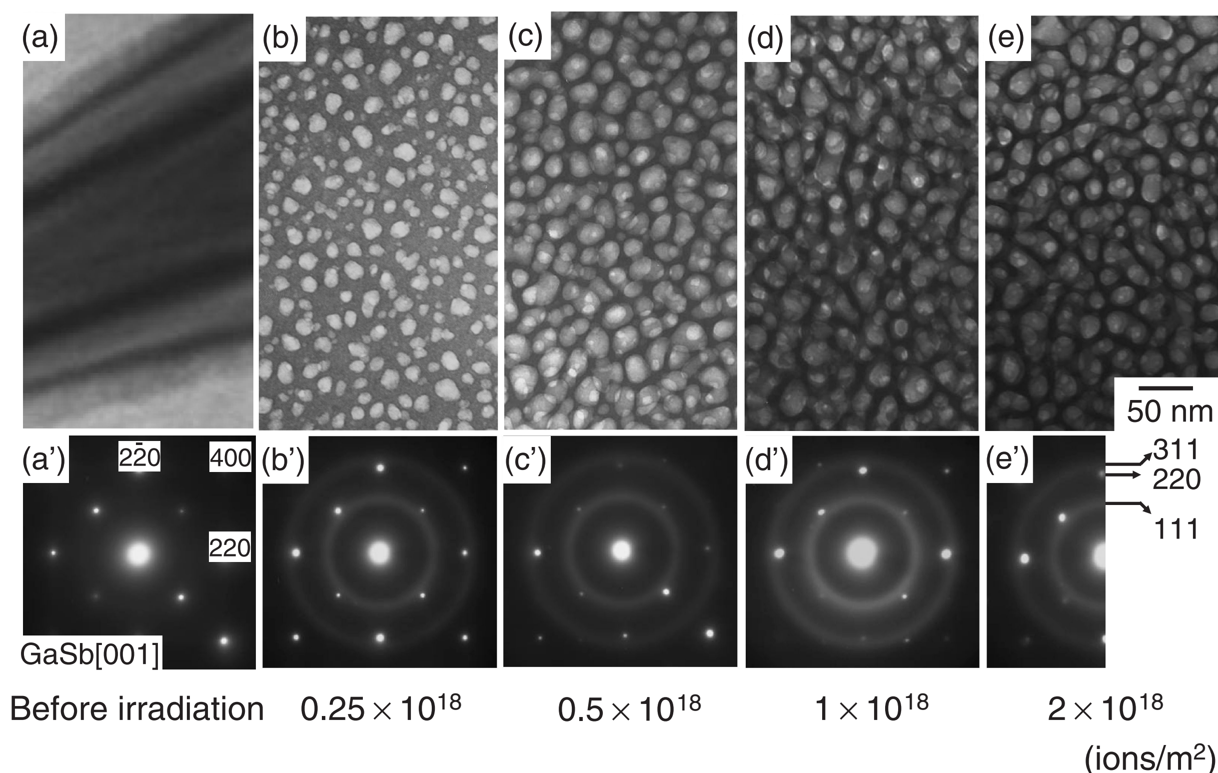

Fig. 1 TEM images (bright-field image) and their SAED patterns of GaSb before and after irradiation.

imately 1.5 dpa). The average diameter, density, and swelling ratio of the voids were about 22 nm, 2×10^{15} voids/m^2, and 24% (a damage level of approximately 3 dpa) in the 1×10^{18} ions/m^2 sample (Fig. 1(d)), and about 21 nm, 2×10^{15} voids/m^2, and 17% (a damage level of approximately 6 dpa) in the 2×10^{18} ions/m^2 sample (Fig. 1(e)), respectively. With increasing ion fluence, the diameter of the voids increased under low irradiation fluences. However, the diameter did not change significantly under high irradiation fluences. It is considered that newly formed voids play a role in the surface sink. The formed interstitials and vacancies escape to the void surface; therefore, voids dose not grow under high irradiation fluences. The Debye-Scherrer rings were observed in the SAED patterns. These rings can be indexed as the 111, 220, and 311 reflections of crystalline GaSb. The structure became polycrystalline after ion irradiation.

Figure 2 shows TEM images (bright-field image) and their SAED patterns of InSb before and after irradiation. The inset is an enlarged view of the 200 diffraction spot. The average diameter of the voids was about 20 nm in the sample irradiated to a fluence of 0.25×10^{18} ions/m^2 (Fig. 2(b)). The density of voids was 2×10^{15} voids/m^2. The swelling ratio of voids was 16%. In the sample irradiated to a fluence of 0.5×10^{18} ions/m^2 (Fig. 2(c)), the diameter of voids grew to 26 nm. The density of voids was 1×10^{15} voids/m^2. The swelling of voids was 19%. The average diameter, density, and swelling ratio of the voids were about 26 nm, 1×10^{15} voids/m^2, and 17% in the 1×10^{18} ions/m^2 sample (Fig. 2(d)), and about 29 nm, 1×10^{15} voids/m^2, and 22% in the 2×10^{18} ions/m^2 sample (Fig. 2(e)), respectively. There is the same as that tendency of GaSb under low and high irradiation fluences. The Debye-Scherrer rings were also observed in the SAED patterns. In the sample irradiated to a fluence of 2×10^{18} ions/m^2, the width of the Debye-Scherrer rings is broad compared with that of GaSb. The 200 superlattice reflections in the [001] net pattern of InSb are almost absent. This indicated that chemical disordering was induced by the irradiation of InSb. Additionally, the streak pattern along the $\langle 110 \rangle$ direction was observed around 200 superlattice reflections, which was slightly rotated from the original direction.

Changes in the diameter of voids in GaSb and InSb as a function of ion fluence are shown in Fig. 3. The void size in InSb is larger than that in GaSb. The void size of InSb irradiated to a fluence of 0.25×10^{18} ions/m^2 is 1.4 times larger than that in GaSb. The number of vacancies in GaSb and InSb are obtained using the SRIM code simulation.[28] Here we adopted the values of displacement threshold energy obtained by Thommen[29] for GaSb (6.2 eV for Ga and 7.5 eV for Sb), and by Bauerlein[30] for InSb (5.8 eV for In and 6.8 eV for Sb). The calculated average production of vacancies per 60 keV Sn^+ ion is about 4450 in GaSb and 4980 in InSb. The local vacancy concentration in InSb is 1.2 times as high as that in GaSb. The large void is explained on the basis of the results of the quantitative evaluation of vacancies existing in InSb. The enthalpy of formation (ΔH) is -42 kJ/mol in GaSb and -31 kJ/mol in InSb.[31] It is also explained that the vacancy concentration in InSb is much higher than that in GaSb. Furthermore, the atomic diffusion by irradiation has been studied intensively by many researches (for example, see Refs. 32) and 33)). The irradiation-induced diffusion is the positional exchange between an atom and a vacancy induced by irradiation, therefore, the rate of migration

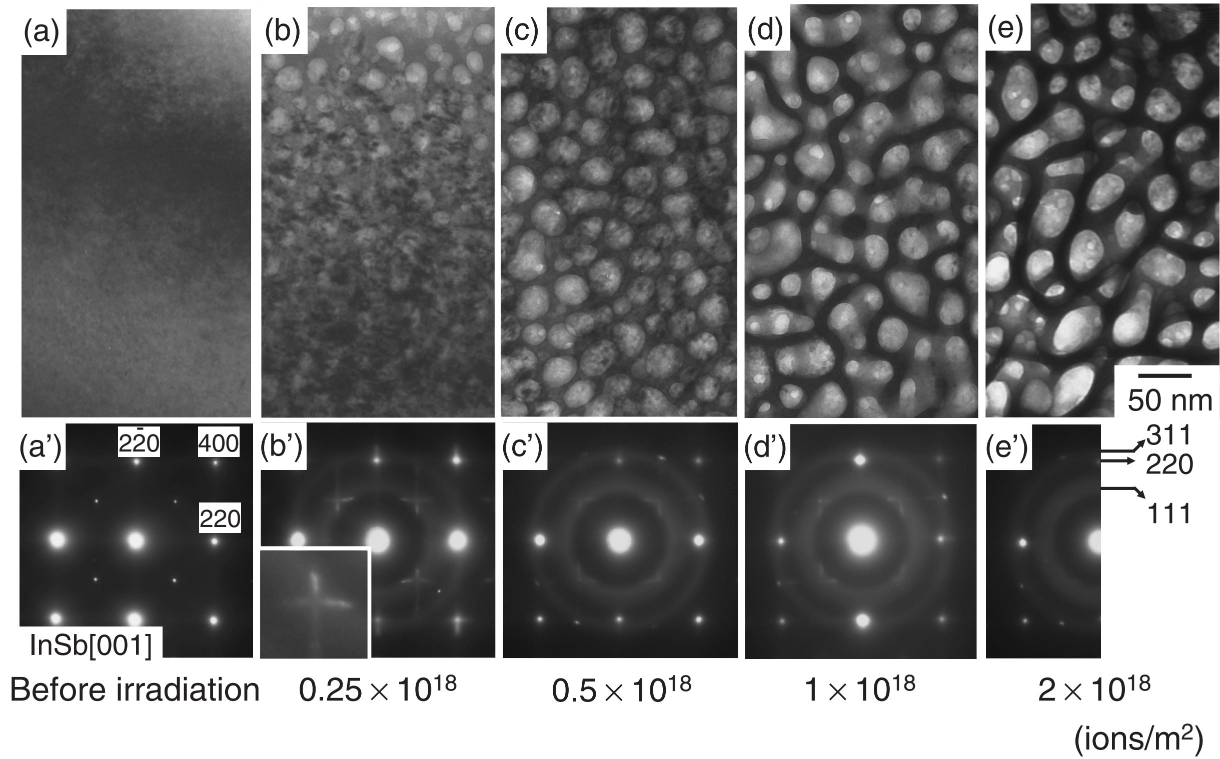

Fig. 2 TEM images (bright-field image) and their SAED patterns of InSb before and after irradiation. The inset is an enlarged view of the 200 diffraction spot.

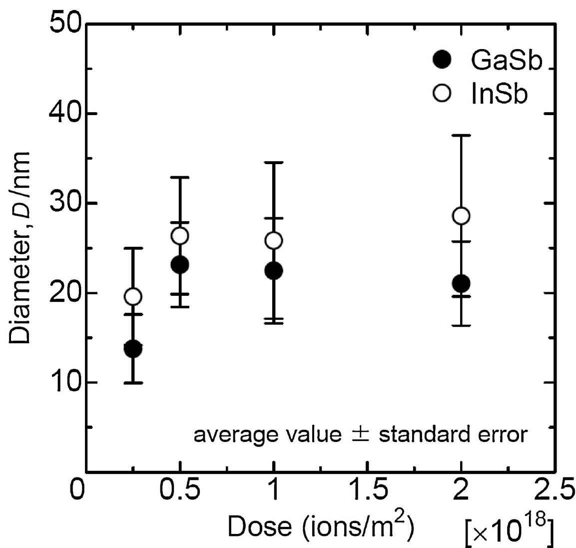

Fig. 3 Changes in void diameter of GaSb and InSb as a function of ion fluence.

strongly depends on the vacancy concentration and its inhomogeneous distribution. The concentration of vacancy in InSb is higher than that in GaSb. It is expected that the irradiation-induced diffusion in InSb is faster than that in GaSb. The relation between atomic diffusion and diameter of void has been showed by Hishinuma *et al.*[34] The solution treated Type 316 stainless steel was 1 MeV electron irradiated at 643–903 K. With increasing irradiated temperature, the void size is increased. It shows that the migration of the point defect enhances the growth of void. Those results may be adapted in irradiated GaSb and InSb. It is also explained that the diameter of the voids in InSb is larger than that in GaSb.

Figure 4 shows an example of high resolution (HR) images and their corresponding fast Fourier transform (FFT) patterns of InSb irradiated to a fluence of 0.25×10^{18} ions/m^2. The local crystal structure in InSb is analyzed by FFT of the HR images to investigate the streak pattern in Fig. 2, since the diameter of the SAED aperture installed in the TEM is too large to obtain the local diffraction pattern. The analysis region is 25 nm × 25 nm. The direction of observation is [001]. In the FFT patterns, many diffraction spots were observed around 200 superlattice reflections. The fluctuation confirmed the location of the diffraction spots. It became evident that the streak pattern is an accumulation of those spots. Figure 5 shows schematic illustrations of (a) a diffraction pattern around the 200 superlattice reflection and (b) an anti phase boundary in a zincblende structure. It is well known that the quadruple satellite spots around superlattice reflections obtained the electron diffraction analysis are for quenched CuAu II alloy.[35] The phenomena could be clearly interpreted by the formation of anti phase domains. It is considered that the observed spots in Figs. 4(a′)–(c′) are similar to the above phenomena. The parameter M, the size of anti phase domains measured in atomic distance, is given, in general, as a fractional number from diffraction patterns.[35] For example, Fig. 5(b) shows the size of the anti phase domain to be $M = 2$. The streak pattern consisting of many spots is observed in Fig. 2. It indicates that anti phase domains of different lengths are formed by ion irradiation. The streak pattern exists the distances of reciprocal lattice

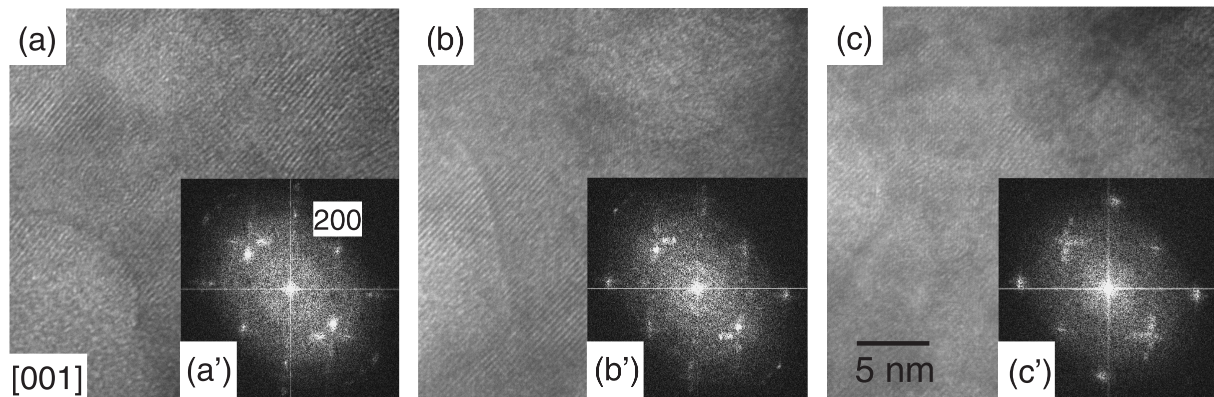

Fig. 4 Example of HR images and their corresponding FFT patterns of InSb irradiated to a fluence of 0.25×10^{18} ions/m^2.

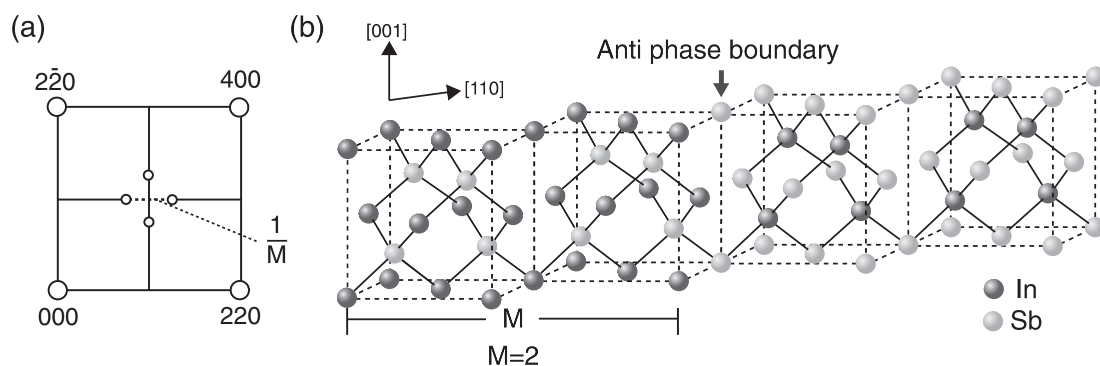

Fig. 5 Schematic illustrations of a diffraction pattern around 200 superlattice reflection and an anti phase boundary in a zincblende structure.

of 1/2–1/12 along the direction of ⟨110⟩. Therefore it is explained that the anti phase boundary introduced random at 2–17 times longer than the InSb unit cell along the direction of ⟨110⟩. This finding indicates that ion irradiation transforms the InSb structure from chemical ordering to chemical disordering via the formation of anti phase boundaries. It is considered that the differences in the void formation and structure change between GaSb and InSb are caused by the difference in the behaviors of point defects. The behavior might be caused by the difference in the stoichiometry of GaSb and InSb.

4. Conclusions

Void formation and structure change induced by heavy ion irradiation in GaSb and InSb have been studied by TEM. The void size in InSb is larger than that in GaSb. The large void is explained on the basis of the results of the quantitative evaluation of vacancies existing in InSb. Ion irradiation transforms the structure of InSb from chemical ordering to chemical disordering via the formation of anti phase boundaries.

Acknowledgments

This work was partially supported by the Iketani Science and Technology Foundation. We would like to thank Dr. M. Imamura, Mr. S. Fujimasa of Kobe University, and Dr. K. Matsumoto of Toyama Prefectural University for useful discussions.

REFERENCES

1) M. G. Grimaldi, B. M. Paine, M.-A. Nicolet and D. K. Sadana: J. Appl. Phys. **52** (1981) 4038–4046.
2) W. G. Opyd, J. F. Gibbones, J. C. Bravman and M. A. Parker: Appl. Phys. Lett. **49** (1986) 974–976.
3) M. Taniwaki, H. Koide, N. Yoshimoto, T. Yoshiie, S. Ohnuki, M. Maeda and K. Sassa: J. Appl. Phys. **67** (1990) 4036–4041.
4) A. Gasparotto, A. Carnera, C. Frigeri, F. Priolo, B. Fraboni, A. Camporese and G. Rossetto: J. Appl. Phys. **85** (1999) 753–760.
5) S. O. Kucheyev, J. S. Williams, C. Jagadish, J. Zou, V. S. J. Craig and G. Li: Appl. Phys. Lett. **77** (2000) 1455–1457.
6) S. O. Kucheyev, J. S. Williams, J. Zou, C. Jagadish and G. Li: Appl. Phys. Lett. **77** (2000) 3577–3579.
7) W. Jiang, Y. Zhang, W. J. Weber, J. Lian and R. C. Ewing: Appl. Phys. Lett. **89** (2006) 021903.
8) I.-T. Bae, W. Jiang, C. Wang, W. J. Weber and Y. Zhang: J. Appl. Phys. **105** (2009) 083514.
9) D. Kleitman and H. J. Yearian: Phys. Rev. **108** (1957) 901.
10) Y. Homma: J. Vac. Sci. Technol. A **5** (1987) 321–326.
11) R. Callec, P. N. Favennce, M. Salvi, H. L'Haridon and M. Gauneau: Appl. Phys. Lett. **59** (1991) 1872–1874.
12) R. Callec and A. Poudoulec: J. Appl. Phys. **73** (1993) 4831–4835.
13) N. Nitta, M. Taniwaki, Y. Hayashi and T. Yoshiie: J. Appl. Phys. **92** (2002) 1799–1802.
14) S. M. Kluth, J. D. F. Gerald and M. C. Ridgway: Appl. Phys. Lett. **86** (2005) 131920.

15) N. Nitta, M. Taniwaki, Y. Hayashi and T. Yoshiie: Physica B **376–377** (2006) 881–885.
16) A. Perez-Bergquist, S. Zhu, K. Sun, X. Xiang, Y. Zhang and L. M. Wang: Small **4** (2008) 1119–1124.
17) N. Nitta, Y. Ohoka, K. Sato, Q. Xu, Y. Hayashi, T. Yoshiie and M. Taniwaki: Mater. Trans. **49** (2008) 1546–1549.
18) S. M. Kluth, D. Llewellyn and M. C. Ridgway: Nucl. Instrum. Methods B **242** (2006) 640–642.
19) I. H. Wilson: J. Appl. Phys. **53** (1982) 1698–1705.
20) B. R. Appleton, O. W. Holland, J. Narayan, O. E. Schow III, J. S. Williams, K. T. Short and E. Lawson: Appl. Phys. Lett. **41** (1982) 711–712.
21) O. W. Holland, B. R. Appleton and J. Narayan: J. Appl. Phys. **54** (1983) 2295–2301.
22) L. M. Wang and R. C. Birtcher: Appl. Phys. Lett. **55** (1989) 2494–2496.
23) L. M. Wang and R. C. Birtcher: Philos. Mag. A **64** (1991) 1209–1223.
24) H. Huber, W. Assmann, S. A. Karamina, A. Mucklich, W. Prusseit, E. Gazis, R. Grotzschel, M. Kokkoris, E. Kossionidis, H. D. Mieskes and R. Vlastou: Nucl. Instrum. Methods B **122** (1997) 542–546.
25) L. Ottavianoa, A. Vernaa, V. Grossia, P. Parissea, S. Pipernoa, M. Passacantandoa, G. Impellizzerib and F. Priolob: Surf. Sci. **601** (2007) 2623–2627.
26) J. Yanagisawa, K. Takarabe, K. Ogushi, K. Gamo and Y. Akasaka: J. Phys. **19** (2007) 445002.
27) S. Koffel, P. Scheiblin, A. Claverie and G. Benassayag: J. Appl. Phys. **105** (2009) 013528.
28) J. P. Biersack and L. G. Haggmark: Nucl. Instrum. Methods **174** (1980) 257–269; J. Ziegler: Software and web site, http://www.SRIM.org.
29) D. Thommen: Phys. Rev. **174** (1968) 938–945.
30) R. Bauerlein: Z. Phys. **176** (1963) 498–509.
31) L. V. Szentpaly: J. Am. Chem. Soc. **130** (2008) 5962–5973.
32) M. Kiritani, N. Yoshida, H. Takata and Y. Maehara: J. Phys. Soc. Jpn. **38** (1975) 1677–1686.
33) J. G. Lee, E. Taguchi and H. Mori: J. Elec. Microsc. **51** (2002) s195–s200.
34) A. Hishinuma, Y. Katano and K. Shiraishi: J. Nucl. Sci. Technol. **14** (1977) 723–730.
35) S. Ogawa and D. Watanabe: J. Phys. Soc. Jpn. **9** (1954) 475–488.